Eur Spine J
DOI 10.1007/s00586-016-4581-6

CASE REPORT

Effects of spine loading in a patient with post-decompression lumbar disc herniation: observations using an open weight-bearing MRI

Niladri Kumar Mahato[1,2] · Daryl Sybert[1,3] · Tim Law[1,4,5,6] · Brian Clark[1,2,6]

Received: 2 November 2015 / Revised: 25 April 2016 / Accepted: 26 April 2016

Abstract
Purpose Our objective was to use an open weight-bearing MRI to identify the effects of different loading conditions on the inter-vertebral anatomy of the lumbar spine in a post-discectomy recurrent lumbar disc herniation patient.
Methods A 43-year-old male with a left-sided L5-S1 post-decompression re-herniation underwent MR imaging in three spine-loading conditions: (1) supine, (2) weight-bearing on standing (WB), and (3) WB with 10 % of body mass axial loading (WB + AL) (5 % through each shoulder). A segmentation-based proprietary software was used to calculate and compare linear dimensions, angles and cross sections across the lumbar spine.
Results The L5 vertebrae showed a 4.6 mm posterior shift at L5-S1 in the supine position that changed to an anterior translation >2.0 mm on WB. The spinal canal sagittal thickness at L5-S1 reduced from supine to WB and WB + AL (13.4, 10.6, 9.5 mm) with corresponding increases of 2.4 and 3.5 mm in the L5-S1 disc protrusion with WB and WB + AL, respectively. Change from supine to WB and WB + AL altered the L5-S1 disc heights (10.2, 8.6, 7.0 mm), left L5-S1 foramen heights (12.9, 11.8, 10.9 mm), L5-S1 segmental angles (10.3°, 2.8°, 4.3°), sacral angles (38.5°, 38.3°, 40.3°), L1–L3–L5 angles (161.4°, 157.1°, 155.1°), and the dural sac cross sectional areas (149, 130, 131 mm^2). Notably, the adjacent L4–L5 segment demonstrated a retro-listhesis >2.3 mm on WB.
Conclusion We observed that with weight-bearing, measurements indicative of spinal canal narrowing could be detected. These findings suggest that further research is warranted to determine the potential utility of weight-bearing MRI in clinical decision-making.

Keywords Back pain · Weight-bearing MRI · Spine motion · Lateral stenosis · Segmentation · Dural sac · Positional MRI

Introduction

Lumbar disc herniation (LDH) secondary to degenerative disc disease is a common occurrence, with as many as 40 % of adults with disc herniation experiencing LDH-induced low back pain (LBP) [1, 2]. Although conservative treatment results in regression of the size of the herniated disc tissue in a good number of cases, about 20 % of LDH patients with unresolved radicular pain require surgical treatment [3, 4]. Around 5–18 % of LDH patients undergoing primary lumbar discectomy and decompression surgery have been observed to develop recurrent lumbar disc herniation (RLDH), arising as a complication from the primary surgery [3, 5, 6]. Typically, RLDH is defined as a recurrence of herniation at the same site of the prior operation, or at the same level on the ipsi- or contralateral

✉ Niladri Kumar Mahato
nm620511@ohio.edu

1 Ohio Musculoskeletal and Neurological Institute (OMNI), Ohio University, Athens, OH, USA

2 Department of Biomedical Sciences, Ohio University, Athens, OH, USA

3 Division of Orthopedic Surgery, OrthoNeuro, New Albany, OH, USA

4 Department of Family Medicine, Ohio University, Athens, OH, USA

5 Clinical and Translational Research Unit, Ohio University, Athens, OH, USA

6 Department of Geriatric Medicine, Ohio University, Athens, OH, USA

Published online: 09 May 2016

side, with at least 6 months of pain-free post-operative period [7, 8].

Different imaging techniques have been used for evaluating primary or secondary disc herniation [9, 10]. Specifically, gadolinium-enhanced magnetic resonance imaging (MRI) with fat saturation, T_1- and T_2-weighted turbo-spin echo and inversion recovery sequences have been used to detect the presence of extruding disc tissue [1, 11]. The decision on surgical intervention in LDH or revision surgeries in RLDH is mostly taken after evaluating the degree of encroachment into the spinal canal and the lateral foramen from protruding disc fragments, as determined by spine imaging in the supine position [3, 8, 12, 13]. However, some studies have reported the use of positional MRI for the quantification of dynamic changes in inter-vertebral anatomy in the supine, sitting and standing positions in symptomatic lumbar stenosis patients [14–16].

While some positional MRI studies have investigated the effects of physiological spine loading on the segmental anatomy and overall lumbar spine curvature in healthy individuals [17–19], a smaller number have examined changes in inter-vertebral morphology in symptomatic LDH patients after axially loading the spine [20–25]. These studies had performed spine loading in the supine position and by using an externally applied, MRI-compatible compression device to analyse changes in spinal canal dimensions and shifts in disc protrusions. Although this external axial loading in the supine position simulated physiological spine compression and demonstrated noticeable dimensional changes in the spine in contrast to conventional supine MRI, some of these results were not in agreement with data obtained from actual weight-bearing radiographic studies [8, 20, 26–28]. Very few studies have utilized positional MR imaging of the spine in weight-bearing positions in lumbar canal stenosis patients [15, 16, 24, 29–33]. Although a few weight-bearing MRI reports are available on non-LBP individuals [19, 23, 29] and on non-specific LBP cohorts [30, 34], to the best of our knowledge, MR image analysis with different axial loading conditions of the lumbar spine in a RLDH patient has not been reported earlier. Accordingly, our objective was to use an open weight-bearing MRI to identify the effects of different loading conditions on the inter-vertebral anatomy of the lumbar spine in a post-discectomy RLDH patient.

Case report

The patient

A 43-year-old male (183 cm, 91 kg,) presented with weakness in the left leg and foot involving the L5-S1 distribution. He had been diagnosed with a left L5-S1 herniation 2 years prior and had undergone a single-level, open discectomy with laminar decompression 1 year prior to reporting to our facilities with symptom recurrence. On a Numeric Pain Rating Scale (1–10), he reported an average score of 7 for the last 7 days prior to the scan, with the pain being most aggravated in the supine position.

MR imaging protocol

The patient was imaged using a G Scan Brio weight-bearing MRI (Esaote S.p.A., Genova, Italy), which is an open-field magnet (0.25 T) with the ability to rotate from supine to a fully upright, weight-bearing (WB) position in 3° increments. The patient was initially imaged in an upright, weight-bearing position (84° tilt of the gantry) with his feet shoulder width apart, strapped securely at his pelvis. This position is recommended in the literature as a safe position that allows optimal WB of the spine without compromising postural stability [35]. Next, the patient was brought to a recumbent position by tilting the table to the horizontal position and imaged in the supine position (0°). Lastly, the patient was imaged again in the WB position while additional loads equivalent to 10 % of his body-weight (9.1 kg) was supported over his shoulders, i.e., containers filled with 5 % of body-weight, placed in two canvass tote bags, and one bag (4.55 kg) was placed over each shoulder, in a weight-bearing + axial loading (WB + AL) position. Sagittal MR images of the entire lumbar spine were acquired at all the three spine-loading conditions using a fast spin echo T_2 sequence (TR = 3520 ms; TE = 125 ms; number of acquisition = 1; matrix = 288 × 234; FOV = 320 × 320; oversampling = 185 %; slice thickness = 4 mm; gap = 1 mm; acquisition time: 4 min 41 s). Scanning time and sequences used for imaging performed in this study were similar to those reported from earlier studies and took less than 5 min of scanning at each position [30]. Scores of 6, 7 and 9 were recorded on the pain rating scale during imaging in the supine, weight-bearing, and weight-bearing + axial loading conditions, respectively. We also acquired additional images of the spine for purposes other than those specified for this study. The total time taken to situate the patient at different positions, allowing ∼5 min before initiating the scan, acquisition of all images and a few minutes of rest in between, was ∼90 min.

MRI analysis

Images were transferred to a proprietary image analysis software system (OrthoCAD, Esaote S.p.A., Genova, Italy). The outlines of all lumbar and the first sacral vertebral bodies including the spinal canal were semi-automatically segmented using the 3D segmentation software. Segmentation was performed across all image slices

Table 1 Lumbar and lumbo-sacral linear (in mm) and angular (in degrees) parameters across the three spine-loading conditions

Linear	Lumbar levels	Supine	Weight-bearing (WB)	Weight-bearing + 10 % body mass (WB + AL)
Inter-vertebral listhesis[a]	L1–L2	2.5	2.4	2.2
	L2–L3	3.3	2.9	2.1
	L3–L4	3.3	2.7	1.8
	L4–L5	3.1	**4.1**	3.8
	L5-S1	**4.6**	3.2	2.9
Inter-vertebral translation[b]	L1–L2	3.0	3.1	3.6
	L2–L3	3.1	3.3	2.5
	L3–L4	2.9	3.9	3.1
	L4–L5	3.2	**5.2**	3.4
	L5-S1	**4.2**	2.1	2
Spinal canal sagittal thickness	*Zone:* L1–L2	13.0	13.08	12.9
	Zone: L2–L3	13.2	14.4	12.4
	Zone: L3–L4	12.2	13.6	12.7
	Zone: L4–L5	13.5	14.3	14.2
	Zone: L5-S1	**13.4**	10.6 (2.4)	**9.5** (3.5)
Disc height	L1–L2	14.06	13.47	13.1
	L2–L3	14.88	14.84	13.54
	L3–L4	15.54	15.14	13.93
	L4–L5	14.98	13.81	13.22
	L5-S1	10.29	8.61	**7.06**
Left intervertebral foramen height	L1–L2	18.21	17.88	15.71
	L2–L3	18.96	17.93	17.09
	L3–L4	19.92	18.16	17.65
	L4–L5	20.74	15.71	16.43
	L5-S1	12.92	10.89	**9.95**

[a] Measured as the distance between the postero-inferior corner of the superior vertebra to the postero-superior corner of the lower vertebra. The *positive values* indicate overhanging of the superior vertebra the inferior one at that level

[b] Measured as the distance between perpendicular planes drawn at the central points of the adjacent vertebrae (see Fig. 1b). *Numbers in parentheses* in *Zone: L5-S1* represent the increase in sagittal-plane posterior disc protrusions measured from the convex disc tips to the perpendicular bisectors drawn to the adjacent L5-S1 vertebral corners with WB and WB + AL (taking the supine value = zero/baseline). Notable changes are represented in *bold*

acquired with one blinded investigator (NKM) segmenting the trials. All images were inspected for disc protrusion, evidence of spine stenosis and lateral foramen narrowing. The software yielded volumetric contour models of the segmented elements of the vertebrae and the spinal canal. Semi-automated quantification of several linear, angular and cross-sectional area (CSA) parameters was performed across all the three loading conditions, and compared. The following parameters were calculated (Tables 1, 2):

- *Inter-vertebral listhesis:* Calculated as the distance between the adjacent corners of contiguous vertebrae in a motion segment (Fig. 1a).
- *Inter-vertebral translation:* Calculated as the distance (on the median bisector) between the perpendicular projections to the centres of two adjacent vertebra drawn from the median bisector of the segmental angle at a given vertebral level (Fig. 1b). This parameter evaluates the relative displacements between adjacent vertebrae relative to its baseline value measured in the supine position (Table 1).
- *Spinal canal sagittal thickness:* The maximum mid-sagittal diameter of the dural sac.
- *Disc height:* Measured at the point of maximum distance between the superior and the inferior end plates.
- *Left intervertebral foramen height:* Measured as the height of the foramen demarcated by the assessor (NKM) over the sagittal images.
- *Intervertebral segmental angles:* The angle between the end plates between adjacent vertebrae.

Table 2 Lumbar and lumbo-sacral angular parameters (in degrees) and cross sectional area (CSA) (in mm^2) dimensions across the three spine-loading conditions

Angular	Lumbar levels	Supine	Weight-bearing (WB)	Weight-bearing + 10 % body mass
Inter-vertebral segmental angles	L1–L2	3.5	8.3	4.0
	L2–L3	2.8	10.7	7.5
	L3–L4	7.3	7.3	9.3
	L4–L5	7.5	12.9	11.2
L5-S1 segmental angle	L5-S1	10.3	**2.8**	4.3
Lordosis angle	L5-S1	53.4	59.2	57.5
Sacral angle	S1	38.5	38.3	40.3
L1–L3–L5 angle	L1–L5	161.4	157.1	155.1
CSA	Lumbar levels	Supine	Weight-bearing (WB)	Weight-bearing + 10 % body-weight
Left inter-vertebral foramen CSA	L1–L2	120	127	121
	L2–L3	101	107	104
	L3–L4	110	115	111
	L4–L5	111	113	118
	L5-S1	106	**98**	100
Spinal canal CSA	*Zone*: L1–L2	155	146	142
	Zone: L2–L3	163	144	138
	Zone: L3–L4	168	143	152
	Zone: L4–L5	164	155	159
	Zone: L5–S1	149	**130**	**131**

Notable changes are represented in *bold*

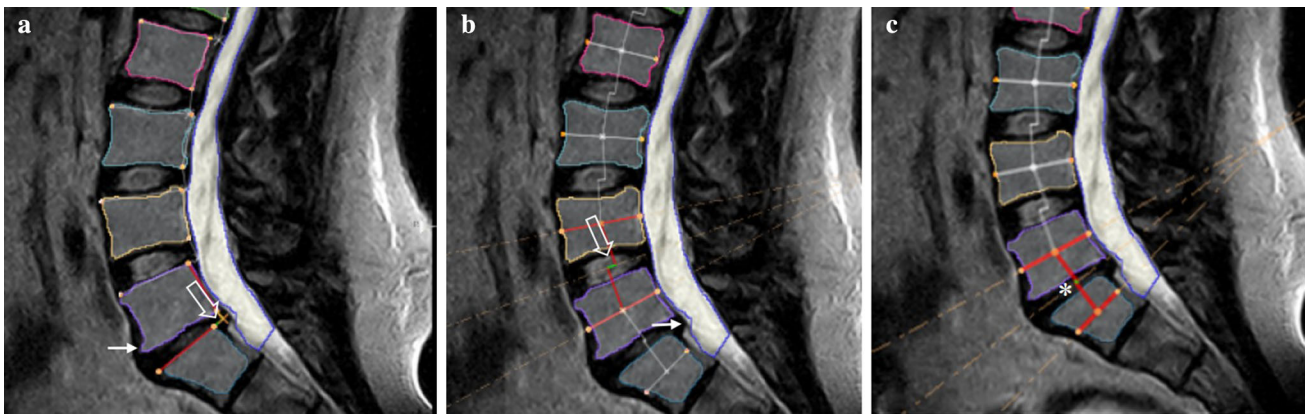

Fig. 1 **a** Sagittal view of the segmented vertebrae in WB. *Open arrow* shows the 'intervertebral listhesis' parameter that is calculated as the distance between the adjacent corners at the posterior ends of contiguous vertebrae. *Arrow* demonstrates the bony spur at the anterior end of the lower vertebral edge of L5. **b** *Open arrow* demonstrates the 'intervertebral translation' parameter calculated as the distance between the two perpendicular projections drawn to the centres of adjacent vertebra from the median bisector of the segmental angle at a given vertebral level (L4–L5, here). The arrow points to the bulging L5-S1 disc on WB. **c** Mid-sagittal WB + AL slice with the *asterisk* showing the L5-S1 disc space

- *L5-S1 segmental angle:* The segmental angle between the adjacent L5-S1 end plates.
- *Lordosis angle:* The angle between the superior plates of L1 and S1.
- *Sacral angle:* The angle between the horizontal plane and the sacral end plate.
- *L1–L3–L5 angle:* The angle formed by the line joining the centres of the L1, L3 and L5 vertebrae.
- *Left inter-vertebral foramen: CSA* Measured as the vertical-plane sectional area of the lateral canals. The area of each foramen was manually demarcated using a pencil tool in the software.

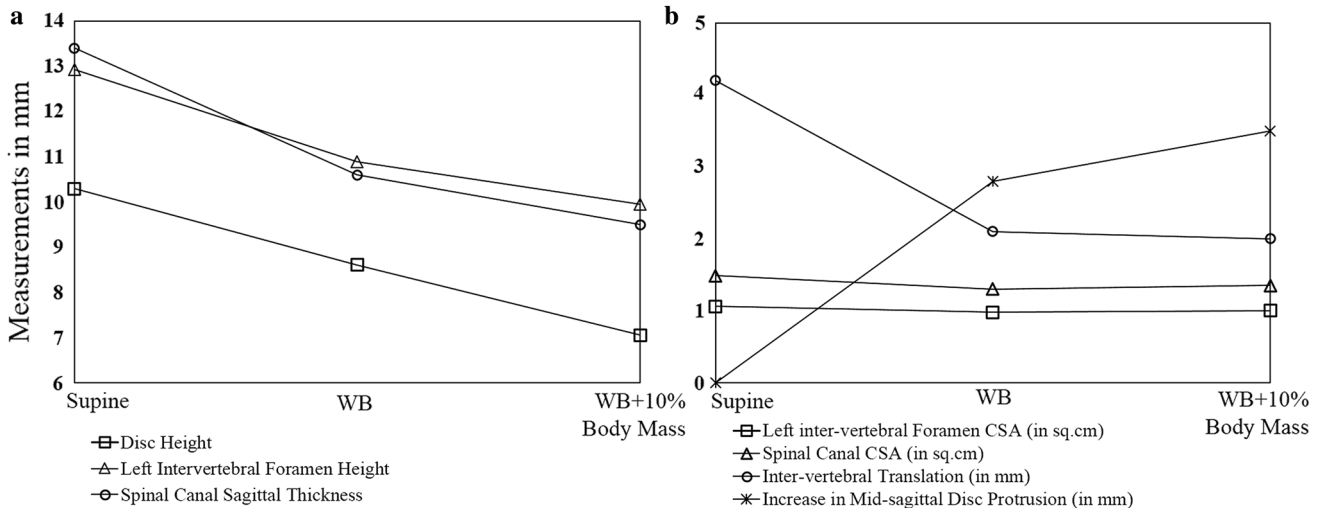

Fig. 2 Parameters as measured at the L5-S1 segment in the supine, WB (weight-bearing) and the WB + AL (weight-bearing and additional loading) conditions. **a** Changes in disc heights, intervertebral foramen height (left side) and L5-S1 spinal canal sagittal thickness. **b** Alterations in L5-S1 left inter-vertebral foramen cross sectional area (CSA) (in cm^2), L5-S1 spinal canal CSA (in cm^2), inter-vertebral translation (in mm), and the change in sagittal-plane posterior disc protrusion (in mm) with WB and WB + AL (taking the value of the supine position = zero/baseline)

- *The spinal canal CSA:* Calculated as the sectional area in the axial plane.

Sagittal-plane protrusion of the L5-S1 disc beyond the posterior limit of the vertebrae was objectively measured using the 'ruler' tool in software (*Zone: L5-S1*, Table 1) and presented as the increase in sagittal-plane posterior disc protrusions measured from the disc-tip to the perpendicular bisectors drawn to the adjacent L5-S1 vertebral corners with WB and WB + AL (taking the value at the supine position = zero/baseline). A new parameter named the absolute vertebral translation (Fig. 1b) was formulated as the displacement (forward or backward) incurred by the superior member of each vertebral segment with the change in spine position from the supine to the WB and then to the WB + AL positions. This 'absolute' translation parameter was calculated assuming the inter-vertebral translation in the supine position to represent a zero displacement. A negative sign to the value indicated a backward translation of the vertebral body and vice versa.

Results

The descriptive statistics observed for all parameters evaluated are displayed in Tables 1 and 2. One of the most prominent findings was a notable posterior shift of the L5 (4.6 mm) on the S1 in the supine position (inter-vertebral listhesis and inter-vertebral translation in Table 1). The L5 shifted anteriorly on standing, and with axial loading of the spine (listhesis: from 4.6 to 3.2 to 2.9 mm). However, the L4 at the L4–L5 junction demonstrated a posterior translation with WB and then a slight anterior shift on WB + AL (listhesis in Table 1: from 3.1 to 4.1 to 3.8 mm). Some other noticeable observations were as follows. (1) Slight increases in spinal canal sagittal thickness at some vertebral levels were noticed on WB (Table 2) [30]. However, marked narrowing of this dimension was noted at the level of L5-S1 junction on WB and with WB + AL (Fig. 2a). (2) Reduction in the L5-S1 left intervertebral foramen height (to <10 mm) with WB + AL. (3) Acute shortening of the L5-S1 angle on standing and reduced disc height at the same level with WB. (4) In comparison to the supine position, the posterior mid-sagittal bulge of the protruding L5-S1 disc demonstrated increases of 2.4 and 3.5 mm with WB and WB + AL, respectively. Lastly, (5) dimensions of the left inter-vertebral foramina CSAs increased slightly with WB at all levels, whereas it was reduced to 98 mm^2 at the L5-S1 space (Fig. 2b), the spinal canal CSA demonstrated critical narrowing (>15 mm^2) [28] at the L5-S1 level from the supine to WB positions (Fig. 2b).

Discussion

This work represents one of the first attempts to quantify changes in inter-vertebral morphology, lateral foramen and spinal canal dimensions in response to physiological loading of the spine, specifically in context of recurrent

disc herniation. We found that, in the supine position, the posterior limit of the L5 vertebra demonstrated a prominent backward shift with relation to the S1 vertebral body, when compared to the WB and WB + AL. This posterior shift of the L5 and reported accentuation of pain may have resulted from the loss of dorsal support elements in the spine secondary to the earlier surgical decompression procedure. This posterior shift of the L5 vertebrae, however, did not alter the spinal canal sagittal thickness nor the CSA possibly due to the absence of the laminae removed with the prior decompression. Marked reduction noticed in L5-S1 disc height on WB and the formation of bony spurs at the anterior edge of the inferior L5 end-pate (Fig. 1b) may be suggestive of segmental instability [36]. Additionally, the L4 vertebra at the adjacent L4–L5 segment demonstrated a paradoxical pattern of displacement. WB resulted in a backward slide of the L4 over the L5 vertebral body, whereas additional loading with the WB + AL resulted in an anterior translation shift of the L4. Altered motion patterns at neighbouring vertebral levels on loading may indicate initial stages of adjacent-segment pathology, as commonly evidenced with LDH or RLDH [24, 37].

Studies with instrumented axial spine loading in the supine position have reported clinically significant (>15 mm^2), multi-level narrowing of the spinal canal in a wide variety of LBP patients using MR imaging, often with re-enactment of the pain during such loading [21, 22, 28]. The range of magnitude and duration of instrumented spine loading in these studies demonstrate large variability. Instrumented spine loading up to 50 % of body-weight and the duration anywhere between 5 and 50 min of standing or additional axial loading have been applied to affect quantifiable deformation of the spinal canal anatomy [23, 28, 29]. In our case study, notable narrowing of the L5-S1 spinal canal CSA, the left lateral foramen CSA, and the left L5-S1 intervertebral foramina heights could be demonstrated with $\sim$10 min of WB. However, only smaller changes were noticed with $\sim$10 min of additional spine loading (i.e., the WB + AL conditioning). In our case, standing alone brought about the critical changes in the canal spaces and accentuation of the disc protrusion. Notable changes were observed when comparing the supine and WB parameters. Since additional L5-S1 disc protrusion, spinal canal dimensions and aberrant L4/L5 translations could be detected comparing the supine and WB images, WB MRI may be considered as an option for the evaluation of crucial parameters required for clinical decision-making.

In summary, we observed that with weight-bearing MRI, measurements indicative of spinal canal narrowing could be detected. These findings suggest that further research is warranted to determine the potential utility of weight-bearing MRI in clinical decision-making.

Compliance with ethical standards

Conflict of interest None of the authors has any potential conflict of interest.

References

1. Cinotti G et al (1998) Ipsilateral recurrent lumbar disc herniation. A prospective, controlled study. J Bone Joint Surg Br 80(5):825–832
2. Peloquin JM et al (2014) Human L3L4 intervertebral disc mean 3D shape, modes of variation, and their relationship to degeneration. J Biomech 47(10):2452–2459
3. Carragee EJ et al (2000) The rates of false-positive lumbar discography in select patients without low back symptoms. Spine (Phila Pa 1976) 25(11):1373–1380 **(discussion 1381)**
4. Connolly ES (1992) Surgery for recurrent lumbar disc herniation. Clin Neurosurg 39:211–216
5. Kambin P et al (1995) Development of degenerative spondylosis of the lumbar spine after partial discectomy. Comparison of laminotomy, discectomy, and posterolateral discectomy. Spine (Phila Pa 1976) 20(5):599–607
6. Suk KS et al (2001) Recurrent lumbar disc herniation: results of operative management. Spine (Phila Pa 1976) 26(6):672–676
7. Erbayraktar S et al (2002) Outcome analysis of reoperations after lumbar discectomies: a report of 22 patients. Kobe J Med Sci 48(1–2):33–41
8. Swartz KR, Trost GR (2003) Recurrent lumbar disc herniation. Neurosurg Focus 15(3):E10
9. Barrera MC et al (2001) Post-operative lumbar spine: comparative study of TSE T2 and turbo-FLAIR sequences vs contrast-enhanced SE T1. Clin Radiol 56(2):133–137
10. Graver V et al (1999) Seven-year clinical follow-up after lumbar disc surgery: results and predictors of outcome. Br J Neurosurg 13(2):178–184
11. Gilbert JW et al (2010) Lumbar disk protrusion rates of symptomatic patients using magnetic resonance imaging. J Manip Physiol Ther 33(8):626–629
12. Lurie JD et al (2013) Magnetic resonance imaging predictors of surgical outcome in patients with lumbar intervertebral disc herniation. Spine (Phila Pa 1976) 38(14):1216–1225
13. Bodiu A (2014) Diagnosis and operatory treatment of the patients with failed back surgery caused by herniated disk relapse. J Med Life 7(4):533–537
14. Beastall J et al (2007) The Dynesys lumbar spinal stabilization system: a preliminary report on positional magnetic resonance imaging findings. Spine (Phila Pa 1976) 32(6):685–690
15. Nandakumar A et al (2010) The increase in dural sac area is maintained at 2 years after X-stop implantation for the treatment of spinal stenosis with no significant alteration in lumbar spine range of movement. Spine J 10(9):762–768
16. Siddiqui M et al (2006) Influence of X Stop on neural foramina and spinal canal area in spinal stenosis. Spine (Phila Pa 1976) 31(25):2958–2962
17. Hirasawa Y et al (2007) Postural changes of the dural sac in the lumbar spines of asymptomatic individuals using positional stand-up magnetic resonance imaging. Spine 32(4):E136–E140
18. Meakin JR et al (2009) The intrinsic shape of the human lumbar spine in the supine, standing and sitting postures: characterization using an active shape model. J Anat 215(2):206–211
19. Meakin JR et al (2008) The effect of axial load on the sagittal plane curvature of the upright human spine in vivo. J Biomech 41(13):2850–2854

20. Ozawa H et al (2012) Dynamic changes in the dural sac cross-sectional area on axial loaded MR imaging: is there a difference between degenerative spondylolisthesis and spinal stenosis? AJNR Am J Neuroradiol 33(6):1191–1197
21. Hiwatashi A et al (2004) Axial loading during MR imaging can influence treatment decision for symptomatic spinal stenosis. AJNR Am J Neuroradiol 25(2):170–174
22. Choi KC et al (2009) Dynamic lumbar spinal stenosis: the usefulness of axial loaded MRI in preoperative evaluation. J Korean Neurosurg Soc 46(3):265–268
23. Jinkins JR, Dworkin JS, Damadian RV (2005) Upright, weight-bearing, dynamic-kinetic MRI of the spine: initial results. Eur Radiol 15(9):1815–1825
24. Ferreiro Perez A et al (2007) Evaluation of intervertebral disc herniation and hypermobile intersegmental instability in symptomatic adult patients undergoing recumbent and upright MRI of the cervical or lumbosacral spines. Eur J Radiol 62(3):444–448
25. Weishaupt D, Boxheimer L (2003) Magnetic resonance imaging of the weight-bearing spine. Semin Musculoskelet Radiol 7(4):277–286
26. Kanno H et al (2015) Axial loading during magnetic resonance imaging in patients with lumbar spinal canal stenosis: does it reproduce the positional change of the dural sac detected by upright myelography? Spine (Phila Pa 1976) 37(16):E985–E992
27. Szypryt EP et al (1988) Diagnosis of lumbar disc protrusion. A comparison between magnetic resonance imaging and radiculography. J Bone Joint Surg Br 70(5):717–722
28. Danielson B, Willen J (2001) Axially loaded magnetic resonance image of the lumbar spine in asymptomatic individuals. Spine (Phila Pa 1976) 26(23):2601–2606
29. Rodriguez-Soto AE et al (2013) Effect of load carriage on lumbar spine kinematics. Spine (Phila Pa 1976) 38(13):E783–E791
30. Tarantino U et al (2013) Lumbar spine MRI in upright position for diagnosing acute and chronic low back pain: statistical analysis of morphological changes. J Orthop Traumatol 14(1):15–22
31. Karadimas EJ et al (2006) Positional MRI changes in supine versus sitting postures in patients with degenerative lumbar spine. J Spinal Disord Tech 19(7):495–500
32. Siddiqui M et al (2006) Effects of X-STOP device on sagittal lumbar spine kinematics in spinal stenosis. J Spinal Disord Tech 19(5):328–333
33. Siddiqui M et al (2005) The positional magnetic resonance imaging changes in the lumbar spine following insertion of a novel interspinous process distraction device. Spine (Phila Pa 1976) 30(23):2677–2682
34. Weishaupt D et al (2000) Positional MR imaging of the lumbar spine: does it demonstrate nerve root compromise not visible at conventional MR imaging? Radiology 215(1):247–253
35. Gallucci M et al (2007) Degenerative disease of the spine. Neuroimaging Clin N Am 17(1):87–103
36. Iguchi T et al (2004) Lumbar instability and clinical symptoms: which is the more critical factor for symptoms: sagittal translation or segment angulation? J Spinal Disord Tech 17(4):284–290
37. Johnsson KE et al (1989) Preoperative and postoperative instability in lumbar spinal stenosis. Spine 14(6):591–593